

# BLOX: The Bonn Lensing, Optical, and X-ray Selected Galaxy Clusters

J. P. Dietrich<sup>1,2</sup>, T. Erben<sup>2</sup>, G. Lamer<sup>3</sup>, P. Schneider<sup>2</sup>, A. Schwobe<sup>3</sup>, J. Hartlap<sup>2</sup>, and M. Maturi<sup>4</sup>

<sup>1</sup>ESO, Garching, Germany, <sup>2</sup>Argelander-Institut für Astronomie, Bonn, Germany, <sup>3</sup>Astrophysikalisches Institut Potsdam, Germany, <sup>4</sup>Institut für Theoretische Astrophysik, Heidelberg, Germany

## Abstract

The mass function of galaxy clusters is an important cosmological probe. Differences in the cluster selection method could potentially lead to biases when determining the mass function. From the optical and X-ray data of the XMM-Newton Follow-Up Survey, we obtained a sample of galaxy cluster candidates using weak gravitational lensing, the optical Postman matched filter method, and a search for extended X-ray sources. We developed our weak-lensing search criteria by testing the performance of the aperture mass statistic on realistic ray-tracing simulations matching our survey parameters. We find that the dominant noise source for our survey is shape noise at almost all significance levels and that spurious cluster detections due to projections of large-scale structures are negligible, except possibly for highly significantly detected peaks. Our full cluster catalog has 155 cluster candidates, 116 found with the Postman matched filter, 59 extended X-ray sources, and 31 shear selected potential clusters. Most of these cluster candidates were not previously known. The present catalog will be a solid foundation for studying possible selection effects in either method. Spectroscopic follow-up observations are underway and we present first results of our follow-up program. The full details of our cluster search are available in Dietrich et al. (2007).

## 1 Introduction

The population of galaxy clusters evolves with redshift, and this evolution depends on the cosmological model. Therefore, the redshift dependence of the cluster abundance can be used as a cosmological test.

Clusters can be selected by various methods: optical, X-ray emission, weak lensing, and – using future surveys – the Sunyaev-Zeldovich effect (SZE). SZE, optical, and X-ray selection of clusters depends on the baryonic content of clusters, which – compared to the predicted dark matter density – is a minor fraction of the clusters' constituents. Optical selection depends on the star formation history, and X-ray and SZE detection requires a hot intra-cluster medium (ICM). Weinberg & Kamionkowski (2002) predict that up to 20% of all weak lensing clusters have not heated their ICM to a level detectable with current X-ray missions. Searching for clusters with SZE is a very promising method but has yet to produce first samples. All four selection methods are sensitive in different redshift regimes. Clearly, no cluster selection method is ideal, and understanding their biases and limitations is important for precision cosmology using clusters.

We conducted a search for galaxy clusters in the public XMM-Newton Follow-Up Survey (XFS, Dietrich et al. 2006) and our private extension to the survey. The XFS is a BVRI survey conducted with WFI@ESO/MPG-2.2 m on 3 sq. deg, which have deep, public XMM-Newton observations. Our private extension covers additional 3 sq. deg. in R-band, of which 2 sq. deg. also have B-band data.

We combine the results of three independent cluster selection methods using the aperture mass statistic (Schneider 1996) for weak lensing selection, the matched filter algorithm of Postman et al. (1996) for optical selection of galaxy clusters, and a search for extended X-ray emission in the XMM-Newton data on our survey fields. The combination allows us to dig deeper into the mass function than we could do with weak lensing selection alone.

## 2 Optical Cluster Search

We chose the matched-filter detection algorithm Postman et al. (1996) because it is well-tested and efficient, it works on single passband catalogs, and can thus be used for the entire area of the XFS. The Postman matched filter method combines positional and photometric information on galaxies by convolving the observed galaxy distribution with a radial and a luminosity filter function. These convolution kernels follow the expected radial distribution and the expected luminosity function of galaxies in a cluster. By appropriately modifying the radial and luminosity filter the matched filter can be tuned to different redshifts.

The matched filter likelihood function is computed on a grid for a set of redshifts. Cluster candidates are peaks in these likelihood maps. A redshift estimate for a cluster candidate is provided by the redshift of the likelihood map in which the cluster likelihood reaches its maximum. We find a total of 116 cluster candidates with the matched filter method. Figure 1 shows the cluster BLOX J1035.9–0331.9 with matched filter likelihood contours as an example. The redshift estimate of the matched filter for this cluster is  $z = 0.4$ .

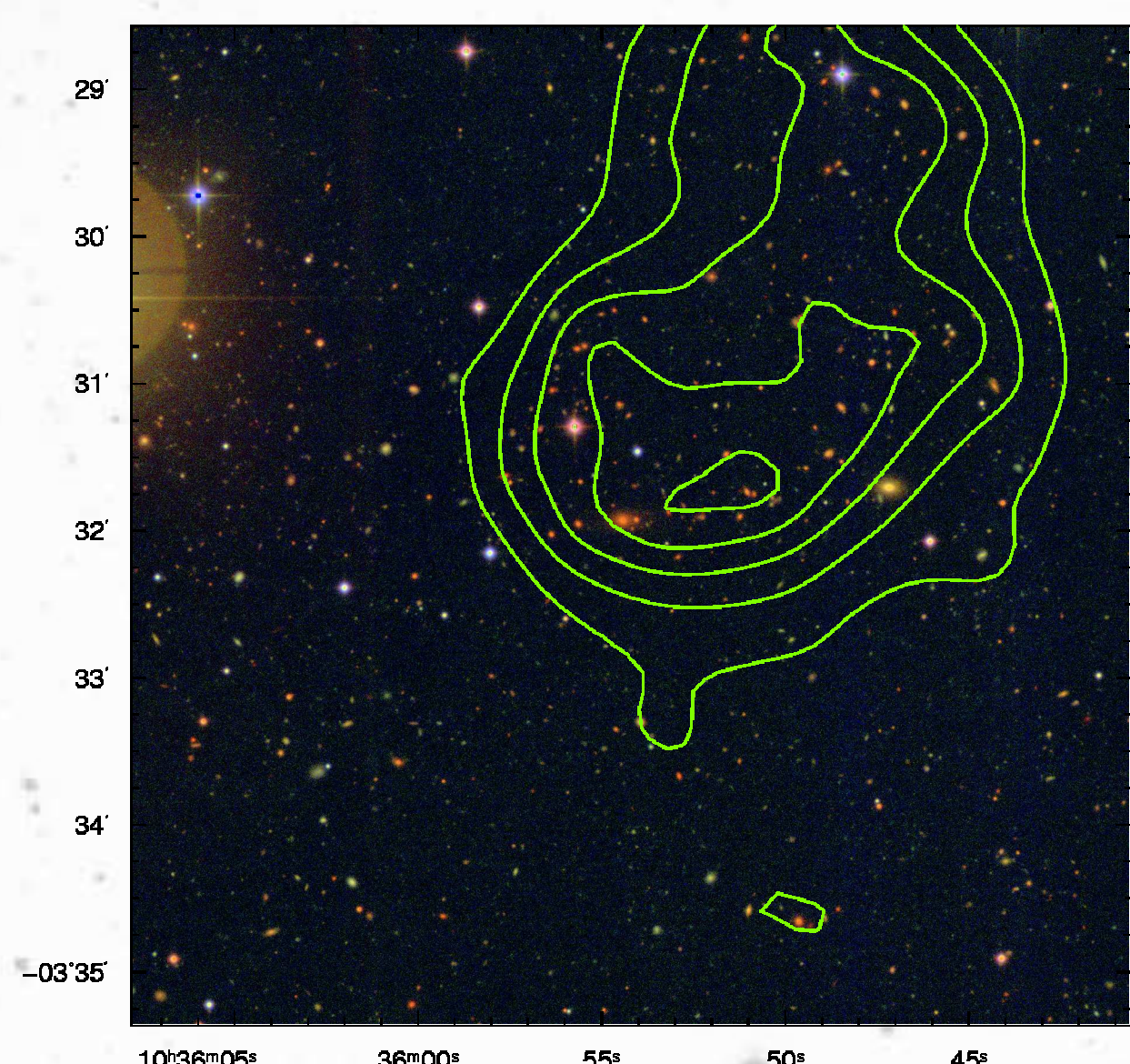


**Figure 1.** Matched filter likelihood contours for the newly detected cluster BLOX J1035.9–0331.9. The small off-set from the BCG may be caused by the large masked area around the bright star north-east of the cluster center. The color image in the background is a BVR composite.

## 3 X-ray Search

The archival XMM-Newton data of the XFS were reduced with the Science Analysis System (SAS). X-ray sources were detected first in local and then in map mode with a box detect algorithm implemented in the SAS task `exboxdetect`. Source lists created in map mode were passed to the SAS task `emldetect`, which performs a simultaneous maximum likelihood multi-source PSF fitting in all energy bands. In our reduction we let `emldetect` fit up to two sources to one source position reported by `exboxdetect`. We found 59 extended X-ray sources, most of which were not previously known galaxy clusters.

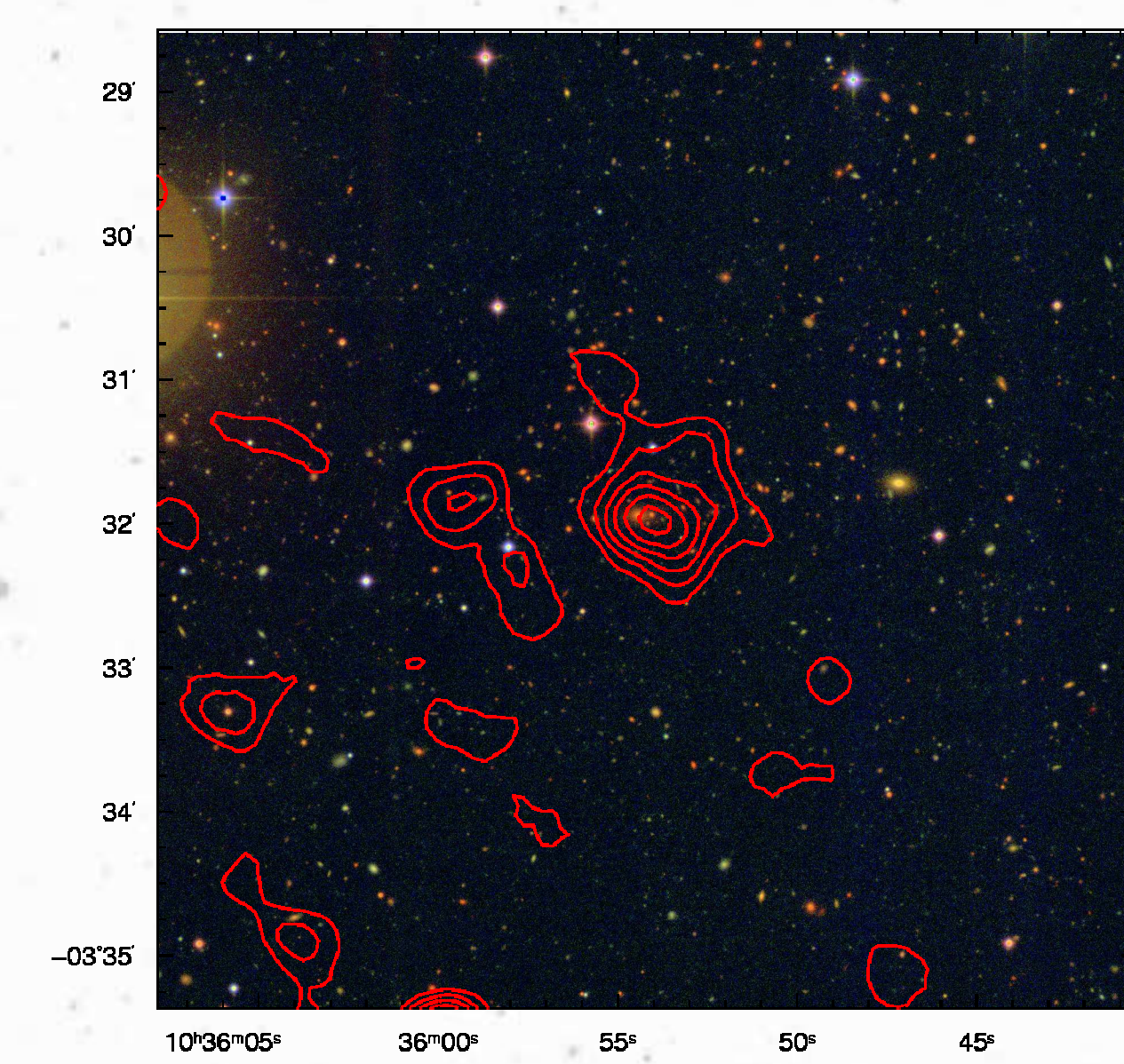


**Figure 2.** Smoothed X-ray contours of the cluster BLOX J1035.9–0331.9.

## 4 Ray-tracing Simulations

We used the aperture mass statistic  $M_{\text{ap}}$  with the filter function proposed by Schirmer et al. (2007) for cluster detection. To study the statistical properties of  $M_{\text{ap}}$  in more detail, we carried out ray-tracing simulations. These were designed to match the survey parameters as closely as possible to provide realistic statistics on the frequency of false positives. For example, we included actual masks from the survey catalogs to simulate the effect of bright stars in the fields.

We computed the aperture mass for 9 different filter scales corresponding to virial radii of  $1000 h_{70}^{-1}$  Mpc to  $2972 h_{70}^{-1}$  Mpc at a redshift of  $z = 0.3$ . We computed  $M_{\text{ap}}$  from the original ray-tracing catalogs and after rotating (1) all galaxies by  $45^\circ$ ; (2) every galaxy by a random angle.

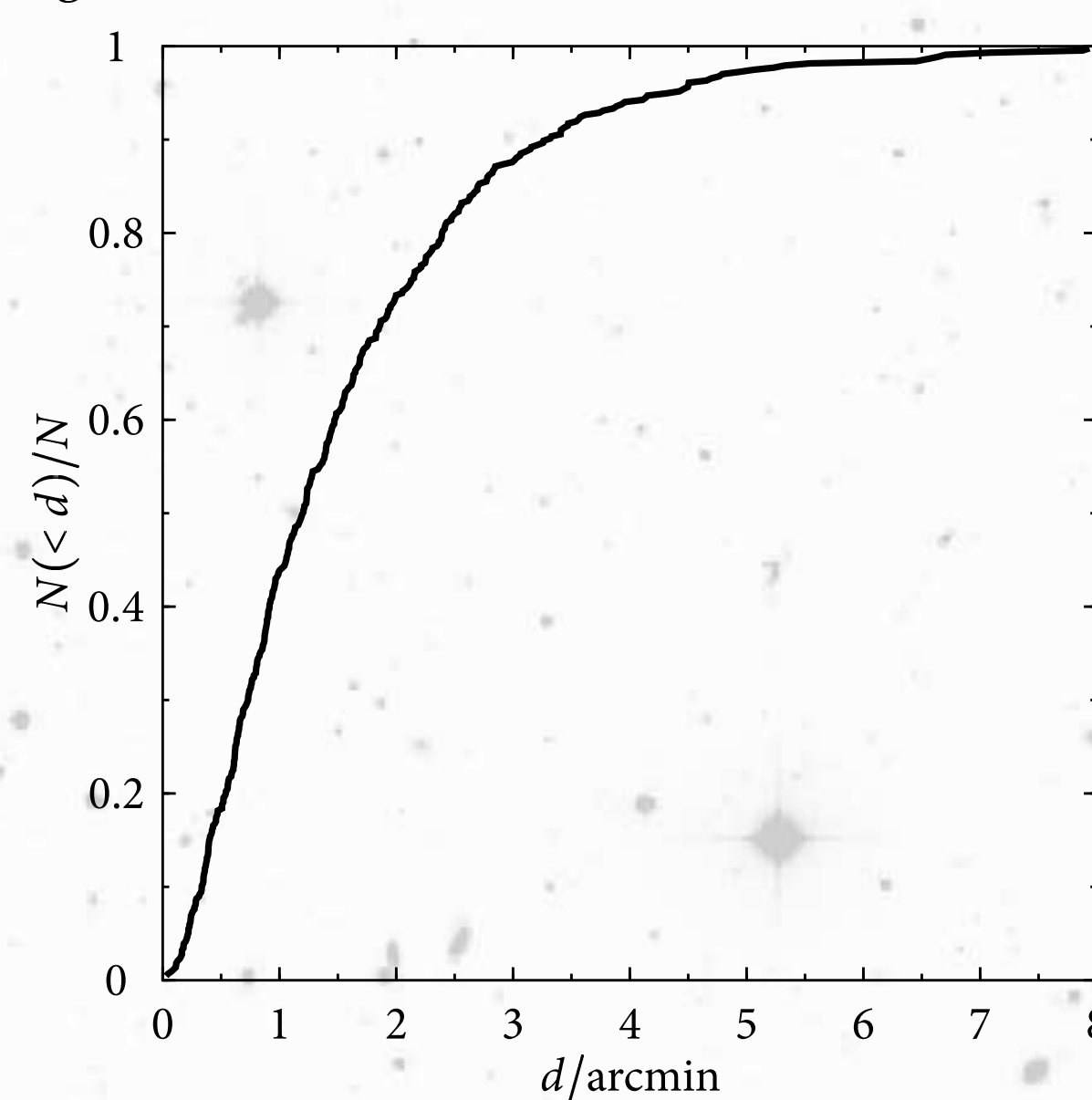


**Figure 3.** Cumulative distance distribution of weak lensing peaks from dark matter halos in our ray-tracing simulations. Statistically, we expected 25% chance alignments. We set the matching radius in the XFS to  $2''.15$ , the radius in which 75% of all matches are made.

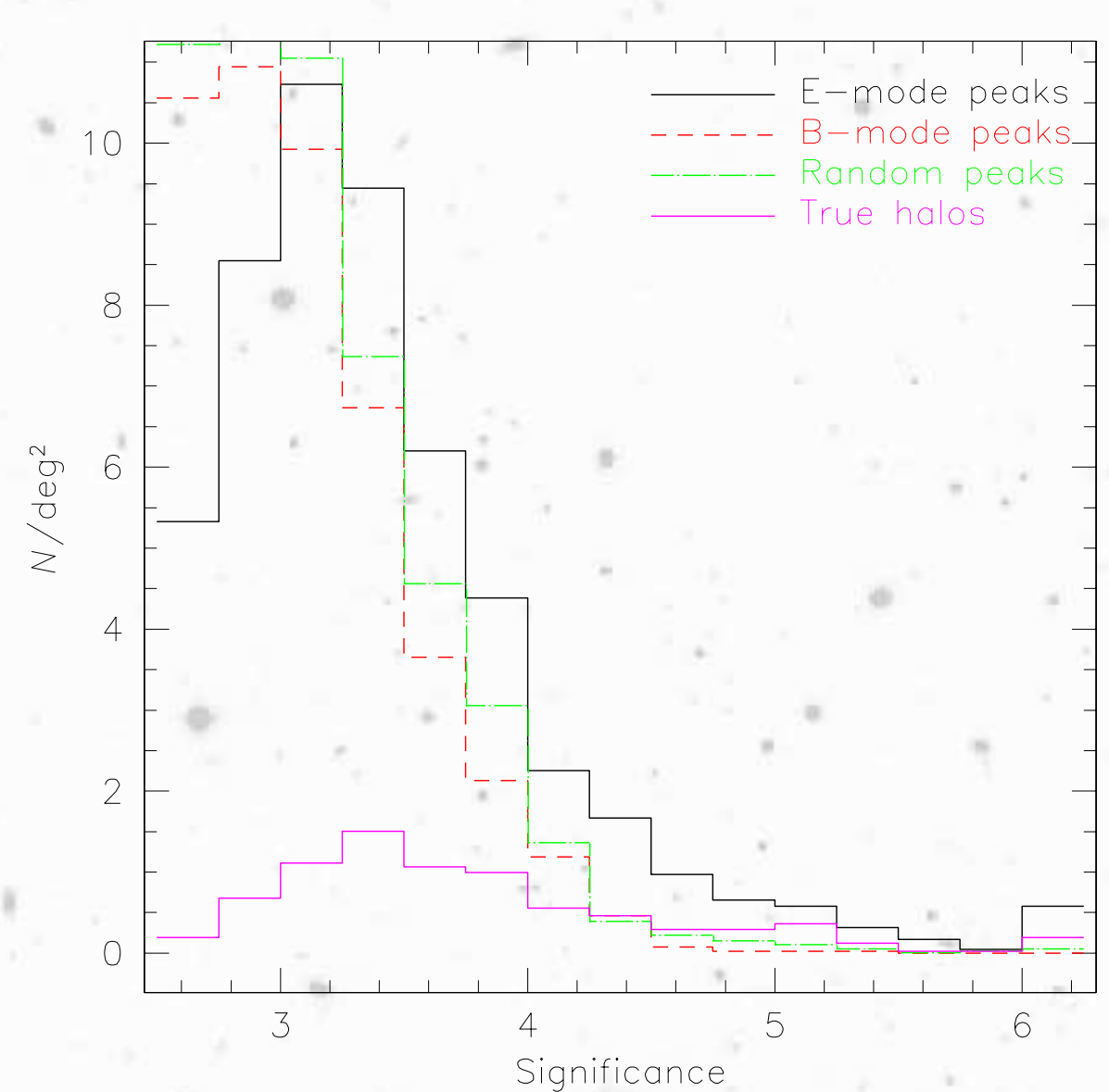


**Figure 4.** Significance distribution for  $M_{\text{ap}}$  peaks in the ray-tracing simulations for E-mode peaks (black), true halos (magenta), B-mode peaks (red), and random peaks (green).

The  $M_{\text{ap}}$  peak significance distribution in Fig. 4 shows that the number E-mode of peaks is higher than the number of any other peak statistic in all significance bins  $> 3.25\sigma$ . The sum of the true halos peaks and the random peaks is compatible with the number of E-mode peaks in the significance bins from  $3.25\sigma$  to  $4.25\sigma$ , if one assumes Poissonian statistics. At higher significances, an excess of E-mode peaks is observed. We surmise that this is due to projections of large-scale structures. This means that we can expect a significant fraction of spurious peaks at almost all significances, a result that is compatible with earlier findings of Hamana et al. (2004) and Hennawi & Spergel (2005). At low significances the spurious peaks will be dominated by shape noise, while at high significances many spurious peaks will be caused by the projection of large-scale structures. We emphasize that the latter class of peaks is in fact caused by gravitational lensing. They just do not correspond to a single mass concentration in 3-d space. These peaks are spurious peaks only in the sense of a galaxy cluster search.

Based on our ray-tracing simulations we set the following detection criteria for weak lensing cluster candidates: Detection significance  $\sigma > 3$ , number of  $M_{\text{ap}}$  filter scales a peak is found in  $n_f > 2$ , and the lensing peak must be within  $2''.15$  from a matched-filter or X-ray candidate or from a cluster (candidate) previously reported in the literature. Lensing peaks with  $\sigma > 5$  are reported in any case.

## 5 Lensing Search

We selected a total of 31 cluster candidates using the aperture mass method on 23 WFI fields, which fulfill the criteria derived from our ray-tracing simulations. On average we find 1.3 weak lensing cluster candidates per XFS field. Most  $M_{\text{ap}}$  peaks do not correspond to a cluster candidate. This is to be expected from the results of our ray-tracing simulations. Twelve of these 31 cluster candidates are previously known cluster (candidates). Eleven of the weak lensing selected clusters were detected with both the matched filter and X-ray emission; 6 of these are previously unknown cluster candidates.

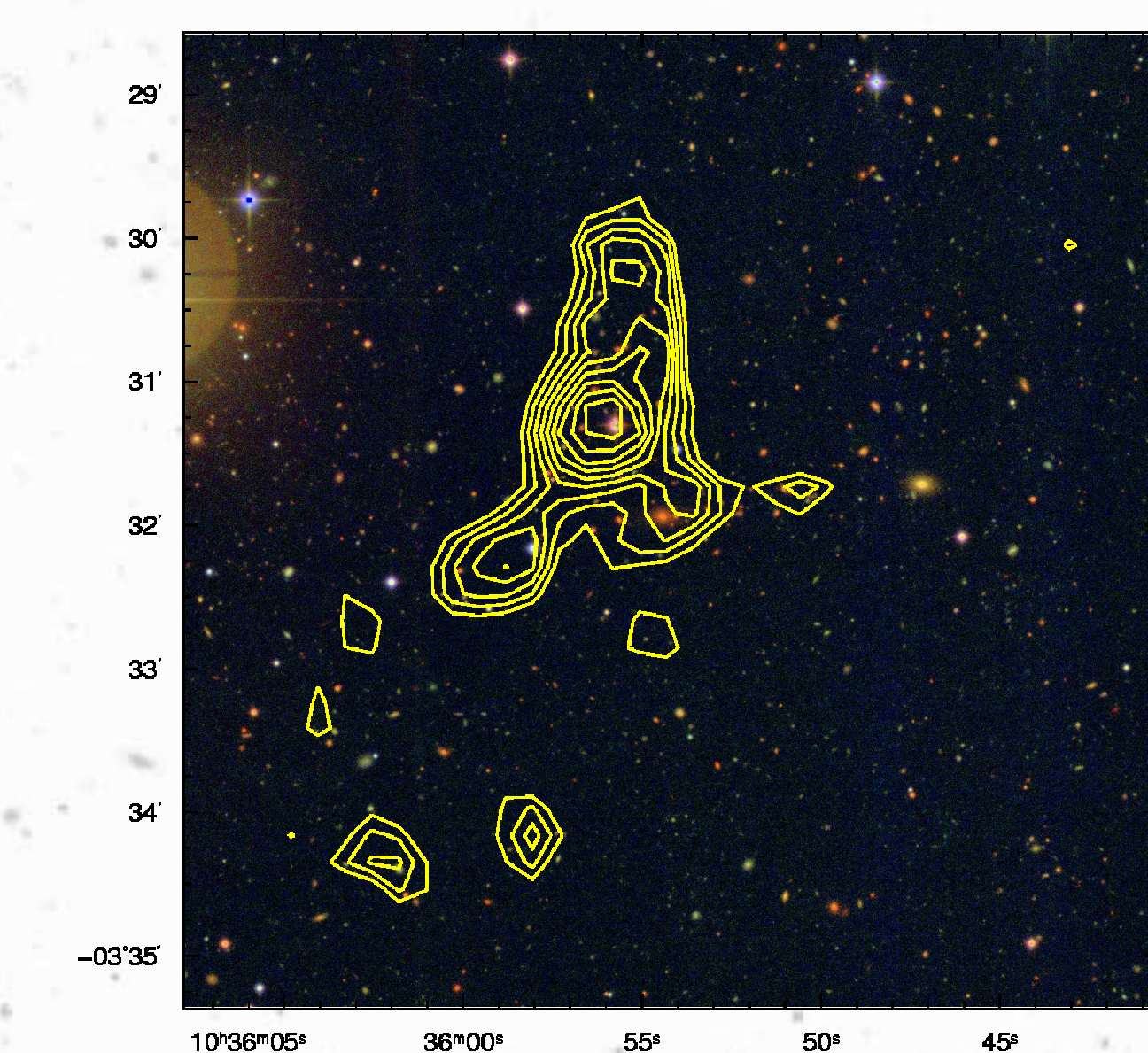


**Figure 5.**  $M_{\text{ap}}$  significance contours for the cluster BLOX J1035.9–0331.9. The peak significance is  $3.7\sigma$ . The observed off-set from the BCG is  $< 1'$  and of the expected size (see also Fig. 3).

The number density of weak-lensing selected cluster candidates is 4.8 per square degree. This is slightly lower than the number density of  $M_{\text{ap}}$  peaks with a halo counterpart in the ray-tracing simulations, which is 6.1/sq. deg. However, the average number density of background galaxies in the XFS data is only  $14.1 \text{ arcmin}^{-2}$ ; this is somewhat lower than in the ray-tracing simulations, which had an average number density of  $16.5 \text{ arcmin}^{-2}$ . Whether the difference in cluster counts can really be attributed to the difference in number density should be checked by adjusting the simulation parameters to match the XFS observations better. The trend to slightly lower number densities is also present if we select only  $M_{\text{ap}}$  peaks with a higher  $\text{SNR} \geq 4$ . The XFS contains 11 of these highly significant peaks associated with a matched filter or X-ray cluster candidate. This corresponds to  $1.7/\text{sq. deg.}$ , compared to  $2.3/\text{sq. deg.}$  in the ray-tracing simulations.

## 6 Spectroscopic Follow-Up

We are carrying out a spectroscopic follow-up program of our cluster sample. The aim of this program is threefold: First, we want to confirm the cluster nature of the weak lensing selected candidates by confirming an overdensity of galaxies in 3-d space. Second, we need the clusters redshift to obtain reliable weak lensing mass estimates. Third, by measuring velocity dispersions, we get another mass proxy that can be compared to weak lensing and X-ray measurements.

To date we have obtained multi-object spectroscopy for about half of our weak lensing sample, plus a few clusters that escape our weak lensing detection. Figure 6 shows the redshift histogram of the cluster BLOX J1035.9–0331.9, a previously unknown cluster at  $z = 0.357$  with a velocity dispersion of  $\sigma = 560^{+100}_{-60} \text{ km s}^{-1}$ .

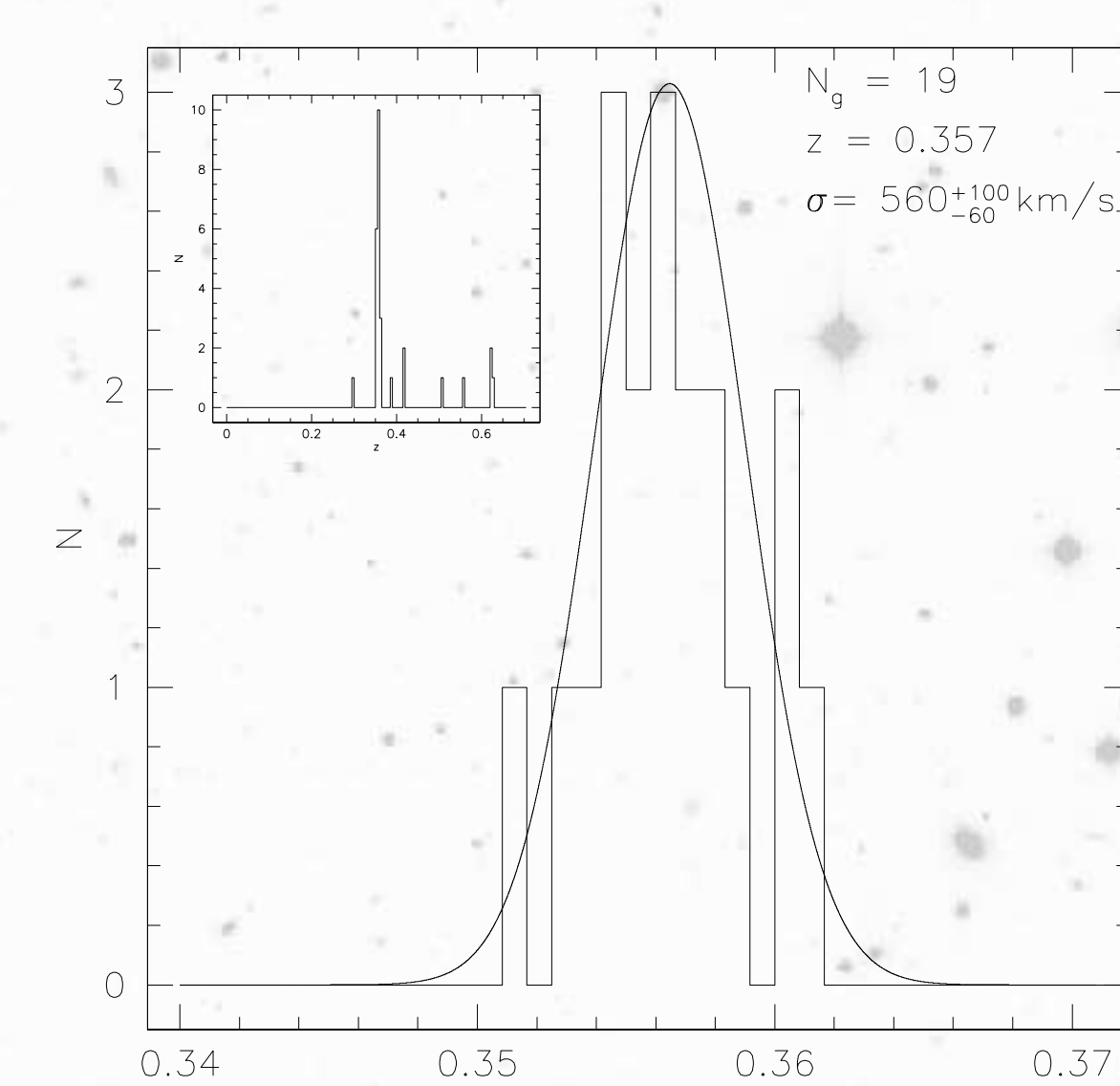


**Figure 6.** Redshift histogram of BLOX J1035.9–0331.9. The inset shows the redshift distribution of all galaxies in the field. The presence of a cluster is clearly confirmed.

## References

- Dietrich, J. P., Erben, T., Lamer, G., et al. 2007, A&A accepted, also arXiv:0705.3455
- Dietrich, J. P., Miralles, J.-M., Olsen, L. F., et al. 2006, A&A, 449, 837
- Hamana, T., Takada, M., & Yoshida, N. 2004, MNRAS, 350, 893 (H04)
- Hennawi, J. F. & Spergel, D. N. 2005, ApJ, 624, 59 (H050)
- Postman, M., Lubin, L. M., Gunn, J. E., et al. 1996, AJ, 111, 615
- Schirmer, M., Erben, T., Hettetscheidt, M., & Schneider, P. 2007, A&A, 462, 875
- Schneider, P. 1996, MNRAS, 283, 837
- Weinberg, N. N. & Kamionkowski, M. 2002, MNRAS, 337, 1269